FINAL

Conf-830659--4

LOW-CYCLE FATIGUE BEHAVIOR OF HT-9 ALLOY IN A FLOWING-LITHIUM ENVIRONMENT*

CONF-830659--4

DE83 014819

O. K. Chopra and D. L. Smith

Materials Science and Technology Division
Argonne National Laboratory
Argonne, Illinois 60439

MASTER

June 1983

DISCLAIMER

To be presented at the Topical Conference on Ferritic Alloys for Use in Nuclear Energy Technologies, Snowbird, Utah, June 19-23, 1983, and for publication in the conference proceedings (TMS-AIME sponsor).

*Work supported by the Office of Fusion Energy, U. S. Department of Energy.

LOW-CYCLE FATIGUE BEHAVIOR OF HT-9 ALLOY IN A FLOWING LITHIUM ENVIRONMENT

O. K. Chopra and D. L. Smith

Materials Science and Technology Division
Argonne National Laboratory
Argonne, Illinois 60439

Low-cycle fatigue data have been obtained on normalized/tempered or lithium-preexposed HT-9 alloy at 755 K in flowing lithium of controlled purity. The results show that the fatigue life of this material decreases with an increase in nitrogen content in lithium. A reduction in strain rate also decreases the fatigue life in high-nitrogen lithium. However, in the range from ~4 x 10^{-4} to 4 x 10^{-2} s^{-1}, the strain rate has no effect on fatigue life in lithium containing <200 wppm nitrogen. The fatigue life of the HT-9 alloy in low-nitrogen lithium is significantly greater than the fatigue life of Fe-9Cr-1Mo steel or Type 403 martensitic steel in air. Furthermore, a 4.0-Ms preexposure to low-nitrogen lithium has no influence on fatigue life. The reduction in fatigue life in high-nitrogen lithium is attributed to internal corrosive attack of the material. The specimens tested in high-nitrogen lithium show internal corrosion along grain and martensitic lathe boundaries and intergranular fracture. This behavior is not observed in specimens tested in low-nitrogen lithium. Results for a constant-load corrosion test in flowing lithium are also presented.

1. INTRODUCTION

Liquid lithium has been proposed as the tritium breeder and/or as a coolant in several fusion reactor concepts. Ferritic steels have been selected as a candidate material for the reactor first-wall/blanket system. The primary incentive for consideration of ferritic steels is their low swelling and high in-reactor creep resistance. Also, the higher thermal conductivity of the ferritic steels provides a reduced thermal stress factor. However, compatibility of the ferritic steels with liquid lithium is a primary feasibility issue for the various liquid metal breeder/coolant blanket concepts.

The cyclic plasma burn projected for some fusion reactor designs will induce severe cyclic thermal stresses in the first-wall/blanket structure. Consequently, the influence of liquid lithium on the fatigue properties is an important consideration in the material selection and design of first-wall/blanket system. Studies on the mechanical behavior of materials in a liquid lithium environment indicate that the compositional and microstructural changes due to selective dissolution or intergranular corrosion may cause degradation of the fatigue properties in lithium (1,2). Low-cycle fatigue data on the HT-9 alloy in a flowing-lithium environment at 755 K (482°C) indicate a strong effect of the concentration of nitrogen in lithium (3). The fatigue life in lithium containing 1000-1500 wppm nitrogen is a factor of 2 to 5 lower than that in lithium with 100-200 wppm nitrogen. The specimens tested in high-nitrogen lithium show extensive internal corrosive attack and partial intergranular fracture. Furthermore, in low-nitrogen lithium, the fatigue life of the HT-9 alloy is independent of strain rate in the range from ~4 x 10^{-4} to 4 x 10^{-2} s^{-1} (2). However, fatigue crack propagation studies on Fe-2 1/4Cr-1Mo ferritic steel in lithium at 673 and 773 K (400 and 500°C) show an increase in crack growth rates (da/dN) at high loading frequencies (4-7). A high density of cleavage-type fracture is observed in lithium. The increased crack growth rates have been explained in terms of a model for strain-rate-induced, liquid-metal embrittlement which considers that embrittlement occurs when the flow stress, increased by high strain rate and low temperatures, exceeds a critical value (6). These studies indicate the importance of lithium purity, temperature, and strain rate on the cyclic properties of materials in lithium.

In addition to cyclic loading, several corrosion studies in lithium have shown that the presence of an applied stress leads to enhanced grain boundary penetration of ferrous alloys (7-9). However, these corrosion tests were conducted in static lithium that was either high in nitrogen or of unknown purity. Consequently, the influence of lithium purity or applied stress on intergranular corrosion of materials in lithium cannot be assessed from these data.

The objective of this paper is to evaluate the effects of a flowing lithium environment on the cyclic properties of the HT-9 alloy as a function of lithium purity, strain rate, and lithium preexposure. Low-cycle fatigue data are presented on normalized and tempered or lithium-exposed HT-9 alloy tested in flowing lithium at 755 K. The corrosive interactions observed under cyclic loading are compared with the results obtained for an HT-9 specimen exposed to flowing lithium with a constant tensile load.

2. EXPERIMENTAL

The test specimens were fabricated from 6.4-mm-diameter rod of HT-9 alloy, Heat 91354. The gauge diameter and length of the fatigue specimens were 2.5 and 6.4 mm, respectively. Tapered gauge-length specimens were used for the constant-load compatibility tests. The gauge section had a total length of 44.5 mm and tapered uniformly from 6.3 to 2.2 mm

in diameter. After fabrication, the specimens were heat-treated in vacuum according to the following schedule: normalize at 1323 K (1050°C) for 1.8 ks and air cool, then temper at 1053 K (780°C) for 9.0 ks and air cool. The fatigue specimens were preexposed for 4.0 Ms at 755 K in flowing lithium containing ~50 wppm nitrogen.

The fatigue tests were conducted in a forced-circulation lithium loop equipped with three test vessels and a cold-trap purification system to control the concentration of nonmetallic elements, e.g., N, C, and H. The quantity of lithium in the loop was ~20 liters, and the lithium within the test vessel was recirculated at ~1 liter/min. The cold-trap temperature was maintained at ~498 K (225°C). Hot trapping with Ti or Zr foils (or use of dissolved getters) was used to reduce the nitrogen level to ~50 wppm in lithium, which is considerably below that attainable by cold trapping. During the tests, the concentration of carbon and hydrogen in lithium was ~8 and 120 wppm, respectively. All fatigue tests were conducted on an MTS fatigue machine in the axial stroke-control mode with a fully reversed triangular waveform and strain rates in the range from 4×10^{-2} to 4×10^{-4} s^{-1}. The details of the fatigue test facility and the procedure for strain control and strain measurement are given elsewhere (3).

The combined effects of constant stress and liquid lithium environment on the corrosion behavior were investigated by exposing monotonically stressed specimens of the HT-9 alloy to flowing lithium. A schematic of the constant-load test fixture is shown in Fig. 1. The fixture was clamped to the lithium test vessel and the specimen loaded through a pull rod by deadweights.

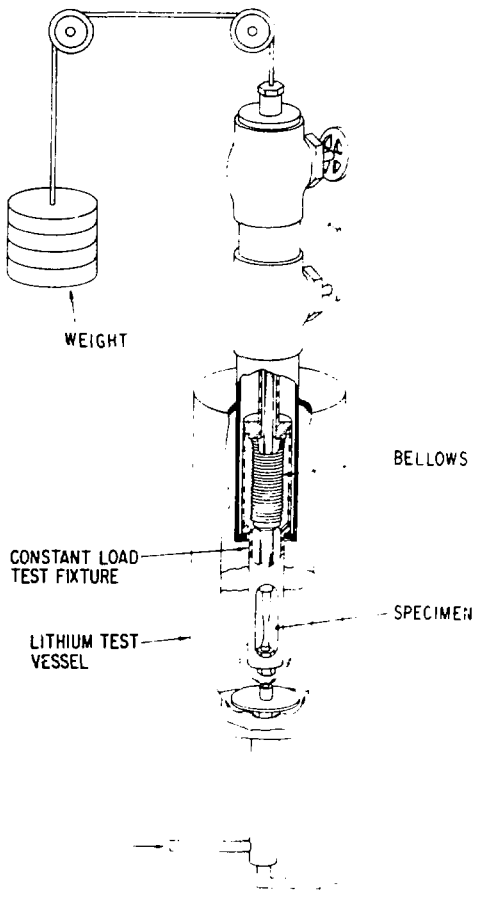

Figure 1 - Schematic of constant-load test facility.

3. RESULTS

Fatigue Tests

The total and plastic strain range vs fatigue life for the HT-9 alloy tested in flowing lithium at 755 K and at different strain rates and lithium purity is shown in Fig. 2. The fatigue strain-life relationship for modified Fe-9Cr-1Mo steel (10) in air at 798-866 K (525-593°C) is also shown in the figure. Fatigue data on the HT-9 alloy in air at temperatures <866 K are not available. However, the cyclic properties of the HT-9 alloy in air should be similar to that of the Fe-9Cr-1Mo steel. The results in lithium show a decrease in fatigue life with an increase in concentration of nitrogen in lithium. For example, the fatigue life in lithium containing <200 wppm nitrogen is a factor of 2-5 greater than in lithium with 1000-1500 wppm nitrogen. A test conducted in lithium with ~560 wppm nitrogen yielded a value of fatigue life of ~60,000 cycles at a total strain range of ~0.55%, compared to ~20,000 and 130,000 cycles, respectively, for the high- and low-nitrogen lithium. The fatigue life in low-oxygen sodium is similar to that in low-nitrogen lithium. Comparison of the fatigue behavior in air and lithium environments indicates that the fatigue life in low-nitrogen lithium is a factor of 2-3 greater than in air.

Fatigue tests conducted in lithium at different strain rates indicate that strain rate in the range from ~4×10^{-4} to 4×10^{-2} s^{-1} has no effect on the fatigue life of the HT-9 alloy in low-nitrogen lithium, i.e., lithium containing <200 wppm nitrogen. At all strain rates, the strain-life behavior follows the data obtained at a strain rate of 4×10^{-3} s^{-1}. However, in high-nitrogen lithium, i.e., lithium with 1000-1500 wppm nitrogen, a change in strain rate from 4×10^{-3} to 4×10^{-4} s^{-1} decreases the fatigue life by a factor of 2.

The data in low-nitrogen lithium at different strain rates can be expressed by a single power-law relationship between plastic strain range, $\Delta\varepsilon_p$, and cycles to failure, N_f, given by

$$\Delta\varepsilon_p = AN_f^{-\alpha}. \qquad (1)$$

The values of the constants A and α were determined from a linear least-squares analysis and are given in Fig. 2. The relationship between elastic strain range and fatigue life was obtained from the cyclic stress-strain behavior and Eq. (1). Figure 3 shows the cyclic stress-strain behavior of the HT-9 alloy in lithium and sodium environments. The cyclic stress amplitude at half-life, $\Delta\sigma/2$, is expressed in terms of the plastic strain amplitude, $\Delta\varepsilon_p/2$, by the relation

$$\Delta\sigma/2 = k\,(\Delta\varepsilon_p/2)^n. \qquad (2)$$

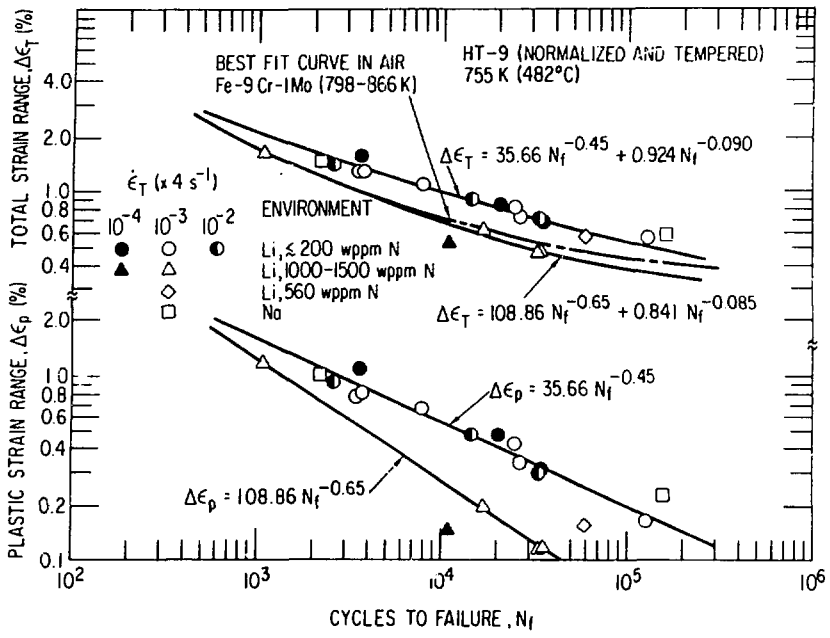

Figure 2 - Total and plastic strain range vs cycles to failure for the HT-9 alloy tested in flowing lithium and sodium at 755 K.

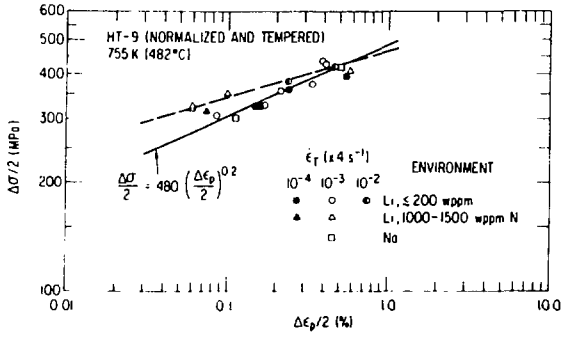

Figure 3 - Cyclic stress-strain relationship for the HT-9 alloy tested in lithium and sodium environments.

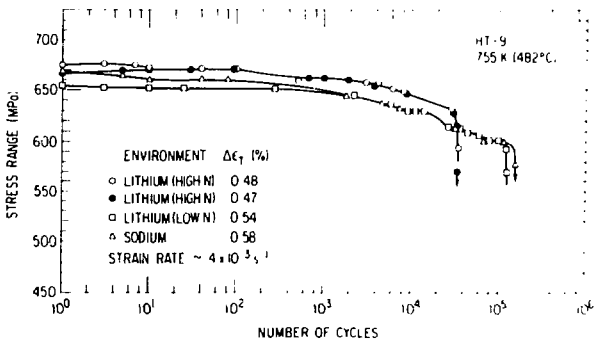

Figure 4 - Cyclic stress range as a function of fatigue cycles for the HT-9 alloy tested in lithium and sodium environments.

At low strain amplitudes, the cyclic stress for the tests in high-nitrogen lithium is higher than that for the tests in low-nitrogen lithium because of the cyclic hardening/softening behavior of the material. The variation in cyclic stress range as a function of fatigue cycles is shown in Fig. 4. After an initial period of ~1000 cycles, during which the cyclic stress was relatively constant, all specimens showed gradual softening for the remaining lifetime. Consequently, for a given strain range, the tests with longer fatigue life, e.g., in sodium or low-nitrogen lithium, show lower values of cyclic stress than the tests with a shorter fatigue life, e.g., in high-nitrogen lithium. The constants k and n in Eq. (2) were obtained separately for the data in high- and low-nitrogen lithium. The best fit lines are shown in Fig. 2.

The relationship between elastic and total strain range and fatigue life can be determined from Eqs. (1) and (2). Thus,

$$\Delta\epsilon_e = \frac{\Delta\sigma}{E} = \frac{2k}{E}\left(\frac{A}{2}\right)^n N_f^{-\alpha n} = BN_f^{-\beta} \qquad (3)$$

and

$$\Delta\epsilon_T = \Delta\epsilon_p + \Delta\epsilon_e = AN_f^{-\alpha} + BN_f^{-\beta}, \qquad (4)$$

where E is Young's modulus. The relationship between total strain and fatigue life is shown in Fig. 2.

The influence of exposure to the lithium environment on the fatigue life of the HT-9 alloy was investigated by conducting tests on specimens that were preexposed at 755 K for 4.0 Ms in flowing lithium containing ~50 ppm nitrogen. Figure 5 shows the strain-life behavior, with and without preexposure, in low-nitrogen lithium at 755 K. The results show that

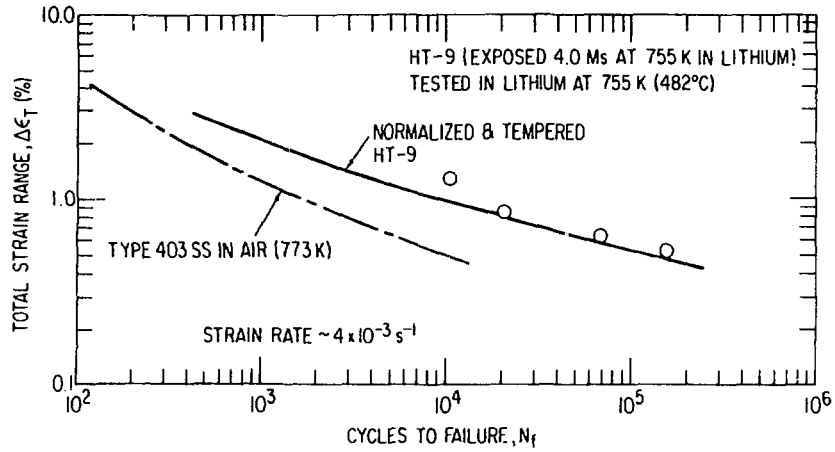

Figure 5 - Effect of lithium preexposure on the fatigue life of the HT-9 alloy tested at 755 K in flowing lithium containing <200 wppm nitrogen.

preexposure of the material to lithium has no effect on fatigue life. Figure 5 also shows a comparison of the strain-life relation of the HT-9 alloy in low-nitrogen lithium with that of Type 403 stainless steel (12Cr martensitic steel) in air at 773 K (11). The fatigue life of the HT-9 alloy in lithium is greater by a factor of 3 to 10.

The test specimens were examined metallographically to evaluate the influence of the test environment on the mode of fracture, surface markings on the gauge section, and internal corrosive attack. Results for fatigue specimens tested at a strain rate of ~4 x 10^{-3} s^{-1} were presented elsewhere (3). The fracture surface of specimens tested in low-nitrogen lithium showed diffuse striations throughout the surface and several ridges extending radially from the region of crack initiation, whereas an intergranular fracture was observed for the specimen tested in high-nitrogen lithium. The gauge sections of the specimens tested in low- or high-nitrogen lithium revealed appreciable corrosion. The surfaces had a pebbled or granular appearance. The specimens tested in high-nitrogen lithium showed internal corrosive attack to a depth of 5-10 μm along the entire gauge length and several intergranular cracks extending as far as 150 μm along the prior austenitic grain boundaries. Internal corrosion or secondary cracks were not observed in specimens (including lithium-preexposed specimens) tested in either low-nitrogen lithium or sodium.

Figure 6 shows micrographs of longitudinal sections of the HT-9 alloy specimens tested in high-nitrogen lithium at strain rates of 4 x 10^{-3} and 4 x 10^{-4} s^{-1}. Although the duration of the slow-strain-rate tests was ~3 times greater, both specimens show internal corrosion to a depth of 5-10 μm and several secondary cracks. The number of cracks is approximately the same for the two tests; however, the cracks extend deeper into the specimen for the slow-strain-rate test, i.e., ~150 and 300 μm at 4 x 10^{-3} and 4 x 10^{-4} s^{-1}, respectively. The effects of internal corrosion are reflected in the mode of fracture. Figure 7 shows the fracture surface of the specimen tested in high-nitrogen lithium at a strain rate of ~4 x 10^{-4} s^{-1}. It shows intergranular fracture near the specimen surface, i.e., the mode of crack propagation is initially intergranular and becomes transgranular after ~350 μm. Internal corrosion or intergranular fracture was not observed in any of the specimens tested in low-nitrogen lithium. The fracture surface of a specimen tested in low-nitrogen lithium at a slow strain rate is shown in Fig. 8. The micrograph shows diffuse striations and ridges extending radially from the region of crack initiation.

Constant-Load Test

The influence of a constant tensile stress on internal corrosion was investigated by exposing a tapered specimen of the HT-9 alloy for 3.6 Ms at 755 K in flowing lithium containing 560 wppm nitrogen. The applied stress was below the yield stress of the material and varied between 136 and 22 MPa. After exposure, several cross sections with different diameters along the length of the specimen were examined to determine the effect of stress on the corrosion behavior. The results indicate that for applied stresses below the yield stress of the material, the corrosion behavior of the HT-9 alloy is independent of stress. Sections of the specimens subjected to different amounts of applied stress show a uniform 7-μm-deep corrosive penetration. Micrographs of the gauge surface and cross section of the specimen are shown in Fig. 9. The gauge surface in contact with lithium has an etched and pebbled appearance and the cross section shows stringers of internal corrosion. The spacing between the stringers is much smaller than the grain size and may correspond to the martensitic lathe boundaries. Electron microprobe analyses indicate a slight depletion of chromium from the specimen surface. The corrosion behavior of the constant-load specimen is similar to the internal corrosive attack observed in the fatigue specimens tested in high-nitrogen lithium. However, the duration of the fatigue tests was significantly smaller, i.e., a maximum of ~0.3 Ms.

4. DISCUSSION AND CONCLUSIONS

Fatigue data in a flowing lithium environment indicate that the most important single parameter in controlling the fatigue properties of the HT-9 alloy is the concentration of nitrogen in lithium. The

$\Delta\epsilon_T$ = 0.48 %, N_f = 34,790, $\dot{\epsilon} \simeq 4 \times 10^{-3}$ s^{-1}

$\Delta\epsilon_T$ = 0.52 %, N_f = 10,910, $\dot{\epsilon} \simeq 4 \times 10^{-4}$ s^{-1}

Figure 6 - Micrographs of longitudinal sections of HT-9 alloy specimens tested in high-nitrogen lithium at 755 K and strain rates of ~4 x 10^{-3} and 4 x 10^{-4} s^{-1}.

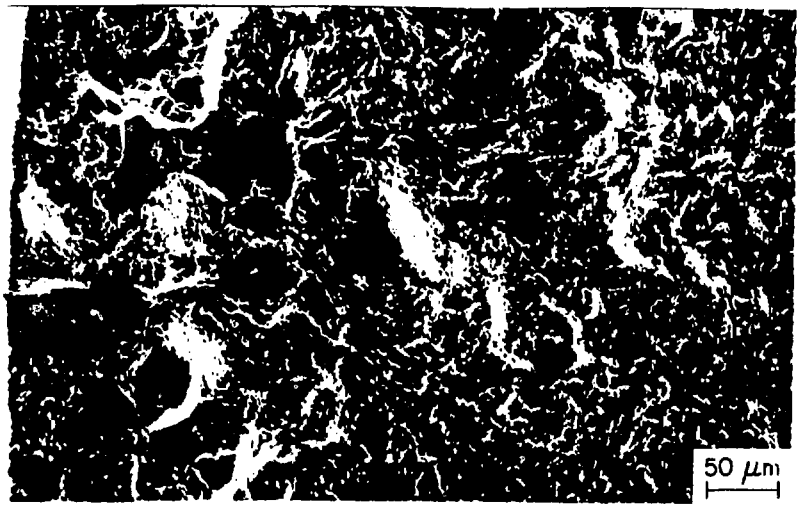

Figure 7 - Micrograph of the fracture surface of the HT-9 alloy tested at 755 K and a strain rate of ~4 x 10^{-4} s^{-1} in lithium containing 1000-1500 wppm nitrogen. The direction of crack propagation is from left to right.

fatigue life in high-nitrogen lithium decreases with an increase in nitrogen content in lithium. In addition, a reduction in strain rate decreases the fatigue life in high-nitrogen lithium. On the other hand, a factor-of-100 change in strain rate has no effect on fatigue life in low-nitrogen lithium, i.e., lithium containing <200 wppm nitrogen. The fatigue life of the HT-9 alloy in low-nitrogen lithium is significantly greater than the fatigue life of modified Fe-9Cr-1Mo steel or Type 403 martensitic steel in air. Furthermore, a 4.0-Ms preexposure to low-nitrogen lithium has no effect on fatigue life. These results indicate that lithium per se has no deleterious effects on the cyclic properties of the HT-9 alloy.

The reduction in fatigue life in high-nitrogen lithium can be attributed to internal corrosive attack of the material. Internal corrosion along grain or martensitic lathe boundaries is not

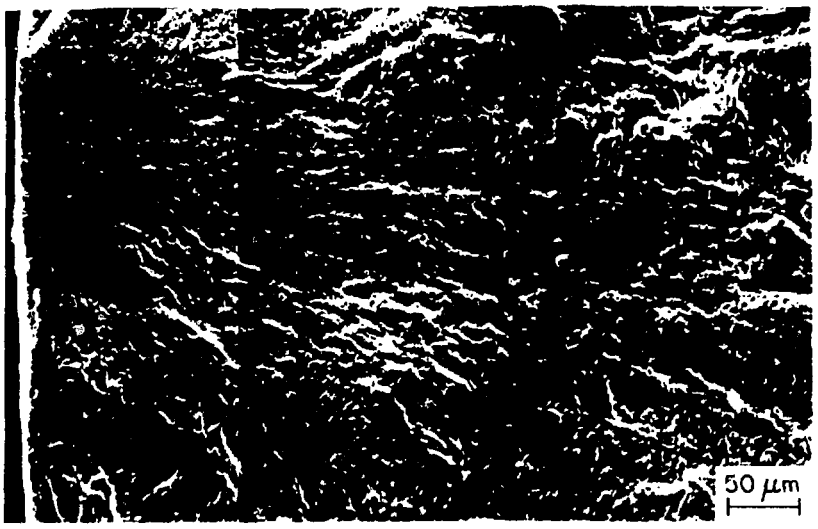

Figure 8 - Micrograph of the fracture surface of the HT-9 alloy tested at 755 K and a strain rate of ~4 x 10^{-4} s^{-1} in lithium containing ~50 wppm nitrogen. The direction of crack propagation is from left to right.

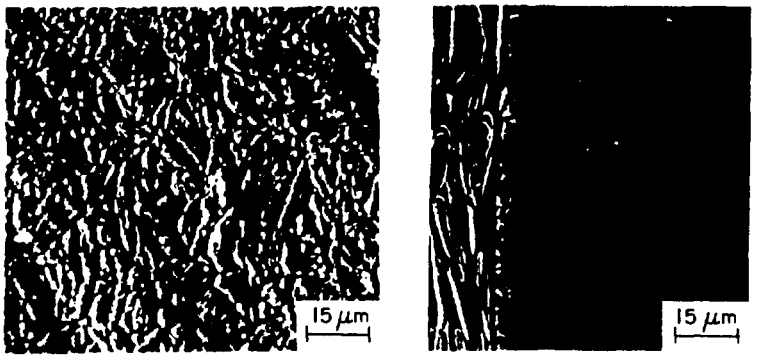

Figure 9 - Micrographs of the (a) gauge surface and (b) cross section of the HT-9 alloy specimen exposed with a constant tensile stress in lithium for 3.6 Ms at 755 K. Concentration nitrogen in lithium was 560 wppm.

observed in corrosion coupons of the HT-9 alloy or Fe-9Cr-1Mo steel exposed to low-nitrogen lithium (12). Selective corrosion along prior austenite grain boundaries and/or martensitic lathe boundaries leads to early crack initiation and thereby reduces fatigue life. The reduction in fatigue life is greater at strain ranges <0.7% because at low strain ranges most of the fatigue life is spent in crack initiation. The internal corrosion in high-nitrogen lithium also results in higher crack propagation rates and intergranular fracture. Such environmental effects are more pronounced at lower strain rates because of greater corrosive attack. Similar behavior has been observed for fatigue crack propagation studies on Fe-2 1/4Cr-1Mo steel in lithium containing ~2000 wppm nitrogen (4,5), namely, a decrease in frequency leads to increased fatigue crack growth rates and intergranular fracture.

Data from the constant-load corrosion tests show that the corrosion behavior of the HT-9 alloy is independent of applied stress for stress values less than the yield stress. These results indicate that the corrosive attack observed for fatigue tests in high-nitrogen lithium is primarily caused by the nitrogen content in lithium and applied stress has little or no effect on corrosion.

A significant result from the fatigue tests in low-nitrogen lithium is that fatigue life is independent of strain rate in the range from ~4 x 10^{-4} to 4 x 10^{-2} s^{-1}. Fatigue crack propagation studies on Fe-2 1/4Cr-1Mo steel in lithium at temperatures <773 K show an increase in crack growth rates with an increase in frequency (4,5). The higher propagation rates at high frequencies are attributed to strain-rate-induced embrittlement (6). At 773 K, the crack propagation rates for Fe-2 1/4Cr-1Mo steel are relatively constant or show a slight reduction with an increase in frequency from ~0.1 to 2 Hz, whereas at higher frequencies the growth rates increase sharply. At 673 K, the crack growth rates

increase at all frequencies >0.1 Hz. The fatigue tests on the HT-9 alloy were conducted in flowing lithium at 755 K and frequencies in the range of ~0.02 and 3 Hz. It is probable that these experimental conditions are outside the range of strain rate and temperature for strain-rate-induced embrittlement of the material. The role of lithium purity on the embrittling effects of the environment is also not established. The fatigue crack propagation tests were conducted in static lithium containing ~2000 wppm nitrogen while the low-cycle fatigue tests were performed in flowing lithium with <200 wppm nitrogen. Fatigue tests in lithium of controlled purity and strain rates >4 x 10^{-2} s^{-1} or temperatures <755 K are required to resolve these issues and establish the environmental effects on the mechanical properties of ferritic steels.

5. ACKNOWLEDGMENT

This work was supported by the Office of Fusion Energy, U. S. Department of Energy.

6. REFERENCES

1. P. F. Tortorelli and O. K. Chopra, "Corrosion and Compatibility Considerations of Liquid Metals for Fusion Reactor Applications," Journal of Nuclear Materials, 103 & 104 (1981) 621-632.
2. O. K. Chopra, "Effects of Sodium and Lithium Environments on Mechanical Properties of Materials," Journal of Nuclear Materials, 115 (1983) 223-238.
3. O. K. Chopra and D. L. Smith, "Effects of Lithium Environment on the Fatigue Properties of Ferritic and Austenitic Steels," Journal of Nuclear Materials, 103 & 104 (1981) 651-656.
4. R. E. Spencer, D. K. Matlock, and D. L. Olson, "The Effects of Liquid Metal Embrittlement on High Temperature Fatigue of 2 1/4Cr-1Mo Steel in Liquid Lithium," Journal of Materials for Energy Systems, in press.
5. D. L. Hammon, G. J. Coubrough, D. K. Matlock, and D. L. Olson, "The Influence of Cyclic Loading on the Lithium Corrosion Behavior of Reactor Materials," Journal of Nuclear Materials, 103 & 104 (1981) 663-668.
6. D. L. Hammon, D. K. Matlock, and D. L. Olson, "Embrittlement of Engineering Materials During High-Temperature Fatigue in a Liquid-Lithium Environment," paper presented at Joint AIME/ASM Meeting, St. Louis, MO, October 1982.
7. D. K. Matlock, R. E. Spencer, D. L. Hammon, T. A. Whipple, and D. L. Olson, "Interrelationship Between Corrosion and Deformation Processes of Materials in Liquid Lithium," Proc. of Second International Conference on Liquid Metal Technology in Energy Production, J. M. Dahlke, ed., CONF-800401-P2 (1980) 22.32-22.39.
8. T. A. Whipple, D. L. Olson, W. L. Bradley, and D. K. Matlock, "Corrosion and Mechanical Behavior of Iron in Liquid Lithium," Nuclear Technology, 39 (1978) 75-83.
9. W. Jordan, W. L. Bradley, and D. L. Olson, "Liquid Lithium Penetration of Stressed Armco Iron," Nuclear Technology, 29 (1976) 209-214.
10. Private communication, V. K. Sikka, Oak Ridge National Laboratory, April 1983.
11. K. Kanazawa, K. Yamaguchi, and K. Kobayashi, "Effects of Temperature and Strain Rate on Low-Cycle Fatigue Properties of 12Cr Martensitic Stainless Steel, SUS 403-B," Trans. of National Research Institute of Metals, 22(1) (1980) 11-18.
12. O. K. Chopra and D. L. Smith, "Corrosion of Structural Alloys in Flowing Lithium and Lead-Lithium Environments," to be presented at the Third Topical Meeting on Fusion Reactor Materials, Albuquerque, NM, September 19-23, 1983.